Organolanthanide-Mediated Ring-Opening Ziegler Polymerization (ROZP) of Methylenecycloalkanes: A Theoretical Mechanistic Investigation of Alternative Mechanisms for Chain Initiation of the Samarocene-Promoted ROZP of 2-Phenyl-1-methylenecyclopropane

Sven Tobisch*[a]

Abstract: A detailed theoretical investigation of alternative mechanisms for chain initiation of the organolanthanide-promoted ring-opening polymerization of 2-phenyl-1-methylenecyclopropane (PhMCP) with an archetypical [Cp_2SmH] model catalyst is presented. Several conceivable pathways for important elementary steps, which also included ring-opening isomerization of PhMCP to phenylbutadienes, were critically scrutinized for a tentative course of the catalytic reaction. The operative mechanism starts with the first *exo*-methylene C=C insertion into the Sm–H bond in a 1,2 fashion and is followed by shift-based β-alkyl eliminative cyclopropyl ring opening by cleavage of a proximal bond, while the alternative mechanism that commences with 2,1-insertion and subsequent ring opening by distal bond scission is revealed to be almost entirely precluded. The facile and irreversible insertion process is not found to occur in a regioselective fashion. The ring-opening process is analyzed as the critical step that discriminates between the two conceivable mechanisms. Opening of the cyclopropyl ring is kinetically easy and proceeds readily for the 1,2-insertion species, while a prohibitively large barrier must be overcome for ring opening of 2,1-insertion species. The isomerization of PhMCP in a ring-opened fashion, which would afford phenylbutadienes as possible products, is predicted to be a less likely process, owing to both kinetic and thermodynamic factors. The phenyl functionality has been demonstrated to distinguish between the regioisomeric ring-opening pathways, both kinetically and thermodynamically, thereby rendering this process selective with regard to the regiochemistry. Overall, chain initiation of the samarocene-mediated ring-opening polymerization of PhMCP is predicted to be a smooth, kinetically facile process.

Keywords: density functional calculations · lanthanides · reaction mechanisms · regioselectivity · ring-opening polymerization

Introduction

Carbon–carbon bond-forming and bond-breaking processes involving methylenecycloalkanes are important synthetic transformations in organic chemistry.[1] The two smallest of these, methylenecyclopropane and methylenecyclobutane, although highly strained,[2] are remarkably stable and readily accessible compounds that display diverse reactivity patterns.[3,4] The release of ring strain by cleavage of the cycloalkane ring is the driving force in numerous organic transformations.[1,3,4]

Increasing attention has been paid to transition-metal-supported reactions of methylenecyclopropanes (MCPs),[5] and efforts have been made to explore viable synthetic routes leading to products with unique properties. In this regard, ring-opening Ziegler polymerization (ROZP) of MCPs is a notable and attractive example, since it affords a novel type of functionalized polyolefins with backbone *exo*-methylene groups [Eq. (1)]. Marks et al. used organolanthanide catalysts in the ring-opening polymerization of MCPs,[6] which has been recently expanded to mono- and disubstitut-

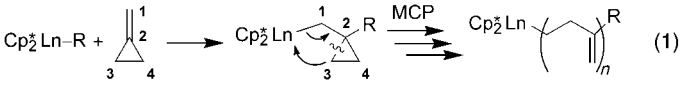

(1)

[a] Priv.-Doz. Dr. S. Tobisch
Institut für Anorganische Chemie
der Martin-Luther-Universität Halle-Wittenberg
Fachbereich Chemie, Kurt-Mothes-Strasse 2
06210 Halle (Germany)
E-mail: tobisch@chemie.uni-halle.de

Supporting information for this article is available on the WWW under http://www.chemeurj.org/ or from the author.

 DOI: 10.1002/chem.200401102

ed derivatives.[7] Furthermore, complexes of late transition metals were shown by Osakada et al. to effect polymerization of MCP (and copolymerization with ethylene or CO) in a ring-opened fashion.[8]

Organolanthanide complexes of the type $[\{Cp^*_2LnH\}_2]$ ($Cp^* = \eta^5$-Me_5C_5; Ln = La, Sm, Lu) have been surveyed with regard to their catalytic capabilities in ring-opening polymerization of methylenecycloalkanes.[6,7] Although only the lutetiocene derivative has been shown to actively promote the homopolymerization of MCP[6b,d] (but, for instance, not of the monosubstituted derivative 2-phenyl-1-methylene-cyclopropane (PhMCP)[7b]), these complexes have been demonstrated to be versatile single-active-site catalysts for copolymerization of both unsubstituted and substituted methylenecycloalkanes with ethylene to afford ring-opened polymers with *exo*-methylene groups.[6,7] Experiments showed that ring-opening polymerization of methylenecycloalkanes is first-order in both substrate and catalyst concentrations,[6d] and proceeds equally well in benzene, toluene, pentane, and related solvents, that is, noncoordinating solvents do not significantly affect the reaction.[6,7] Characterization of homopolymers and ethylene copolymers by NMR spectroscopy and gel-permeation chromatography (GPC) revealed a clean enchainment of MCP and PhMCP in a ring-opened fashion to afford products bearing *exo*-methylene units. These observations, combined with further mechanistic data, strongly argue that polymer growth proceeds through a repeated sequence of 1,2-insertion and ring-opening events.[6b,d,7b]

Scheme 1 displays a general catalytic reaction course for chain initiation of organolanthanide-supported ring-opening MCP polymerization by $[Cp^*_2LnH]$ catalyst **1** comprising the first monomer insertion into the Ln–H bond, subsequent ring opening, and also β-H elimination, which would afford butadiene, that is, the ring-opened MCP isomer, as a possible product. With regard to the regiochemistry, insertion of the olefinic subunit of MCP into the Ln–H bond of **1** can in principle afford two different regioisomers **2** and **3** as a result of respective 1,2- and 2,1-addition. The following ring opening occurs most reasonably via a shift-based β-alkyl eliminative mechanism, which has precedence in β-alkyl elimination as the major chain termination path in organolanthanide, Group 3, and Group 4 metallocene-assisted α-olefin polymerization.[9] This mechanism is further supported by ^{13}C-labeling copolymerization experiments.[6d] Following the 1,2-insertion path, ensuing β-alkyl eliminative cyclopropane ring opening of **2**, which most likely involves cleavage of a proximal (i.e., C^2–C^3 or C^2–C^4) bond of the cyclopropyl ring, affords the ring-opened species **4**, which can easily rearrange into **4′**. Ring opening through distal (i.e., C^3–C^4) bond scission [Eq. (2)] can formally be envisioned as an alternative path. However, this would require an additional transfer of an H atom (i.e., $C^2 \rightarrow C^4$), which indicates this path to be less likely. Compounds **4**, **4′** represent the final points of chain initiation by mechanistic cycle **I** that starts with 1,2-insertion, at which point the process can branch in different directions. First, growth of the polymer chain can occur in a ring-opened fashion by the repeated

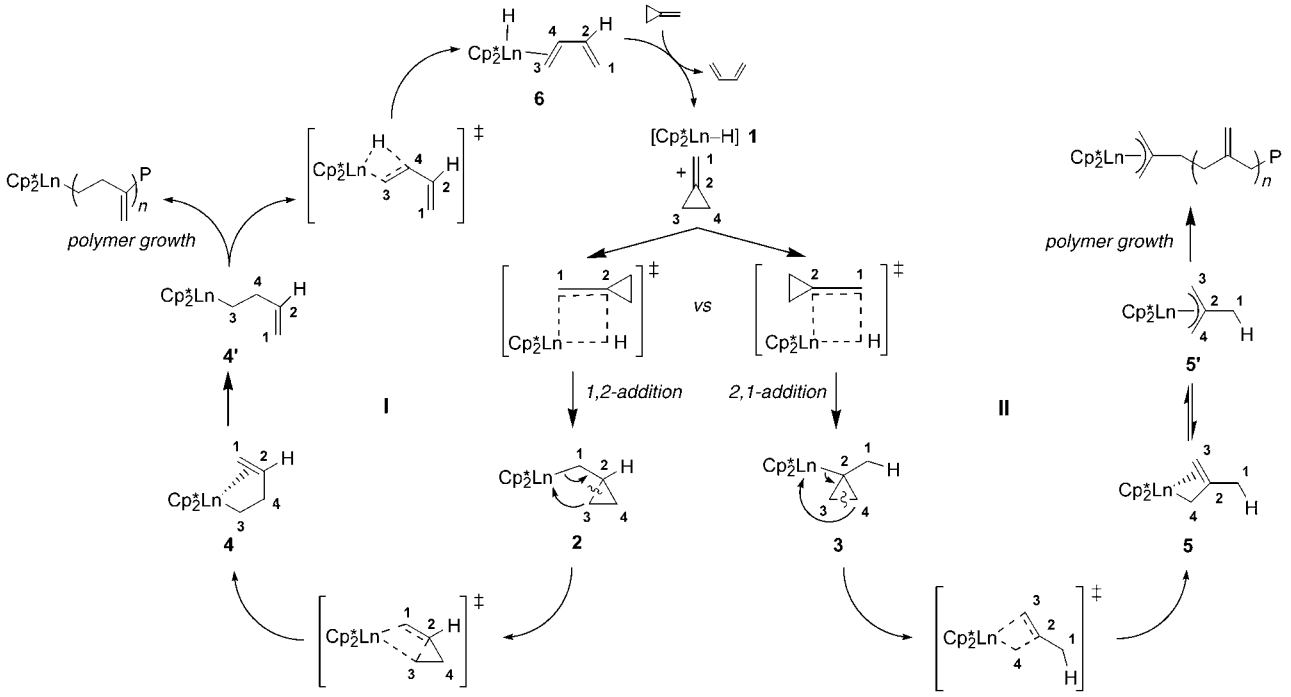

Scheme 1. General catalytic reaction course for chain initiation of organolanthanide-mediated ring-opening Ziegler polymerization of methylenecyclopropane, based on experimental studies of Marks et al.[6,7] The alternative mechanistic cycle **II** for chain initiation starting with 2,1-insertion, although not consistent with experimental mechanistic data,[6b,d,7b] is also included to illustrate the mechanistic diversity.

1,2-insertion of MCP into the Ln–C bond, or **4**, **4′** can undergo β-H elimination, as one of the imaginable paths for chain transfer, giving rise to the 1,3-butadiene–hydride–Ln species **6**. Incoming MCP might displace butadiene from **6** to afford this ring-opened MCP isomer as a side product, thereby initiating a new polymer chain following the **1**+ MCP→**4** sequence of steps. As mentioned above, mechanistic cycle **I**, involving sequential 1,2-insertion (into the Ln–H and Ln–C bonds, respectively, for chain initiation and growth) and β-eliminative shift-based ring-opening events, is operative for the organolanthanide-mediated reaction.

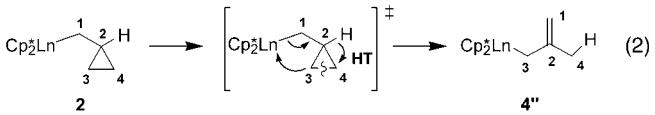

2 **4"** (2)

The alternative mechanistic cycle **II** for chain initiation starting with 2,1-insertion, which has been argued to be effective for the reaction assisted by late transition metals,[8] is also included in Scheme 1 to illustrate the mechanistic diversity. In contrast to **2**→**4** ring opening, the β-alkyl elimination at the cyclopropyl ring in **3** is most likely to take place through distal bond (i.e., C^3–C^4) cleavage, as revealed from labeling experiments and NMR spectroscopic analysis of the polymer product for the Pd-catalyzed process.[8a] This gives rise to a newly formed allylic group in the ring-opened product, which adopts an η^1-σ (**5**) or η^3-π (**5′**) mode of allyl–Ln coordination.[10] Other conceivable paths by proximal bond (i.e., C^2–C^3 or C^2–C^4) scission [Eqs. (3) and (4)] would make additional H-transfer steps necessary and would lead to terminal groups that are not detected experimentally;[8] hence, these paths are less likely.

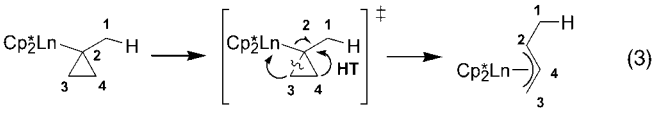

3 **5"** (3)

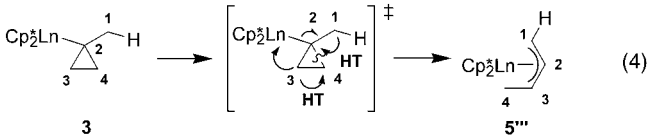

3 **5'''** (4)

For the asymmetrically substituted PhMCP, the course of the polymerization reaction displays greater diversity than for MCP, since in this case alternative pathways are imaginable for each of the elementary steps of the two mechanistic cycles shown in Scheme 1, which are distinguished by the relative orientation of the phenyl group towards the active metal center (vide infra). The arene functionality, through its ability to interact electronically with the electrophilic lanthanide center, might be considered to be a crucial factor in controlling the structure of the polymer product. However, to use this handle efficiently in the process of rational catalyst design, a detailed understanding of its role in the sequence of participating elementary steps is a prerequisite.

Here we present a computational investigation of the salient mechanistic features of the chain-initiation process associated with the ring-opening polymerization of PhMCP mediated by $[\{Cp_2^*LnH\}_2]$ compounds, for which the monomeric species Cp_2SmH was adopted as a realistic catalyst model. This consists of the comprehensive exploration of alternative pathways for the crucial steps of the different mechanisms shown in Scheme 1 and is aimed at extending the mechanistic understanding of the organolanthanide-mediated ring-opening polymerization of MCPs by elucidating the following aspects: 1) Which mechanism is operative for chain initiation in the organolanthanide-mediated ring-opening polymerization of PhMCP? 2) Which factors determine the regioselectivity of the insertion, ring-opening, and β-H elimination steps? 3) Does the weakly Lewis basic aryl substituent stabilize electronically the electrophilic Lewis acidic lanthanide center, how does this interaction affect the energy profile of alternative pathways of the various steps, and can it force these processes to selectively traverse only one of them? 4) Which of the various steps is effective in discriminating between the possible regioisomers of the ring-opened product?

The present computational study is, to the best of our knowledge, the first detailed theoretical mechanistic investigation of the sequence of steps involved in chain initiation associated with ring-opening PhMCP polymerization mediated by the samarocene hydride complex, which is considered to be a prototypical organolanthanide catalyst. The insertion and ring-opening steps for MCP catalyzed by the related Cp_2LaH and Cp_2LuH catalysts has been the subject of recent computational studies.[11a,b] The results and mechanistic conclusions presented here are in sharp contrast to these studies, but this cannot be attributed to the slightly different catalysts and substrates examined.[11c]

Computational Details

All calculations were performed with the program package Turbomole[12] using density functional theory (DFT). The local exchange-correlation potential by Slater[13a,b] and Vosko et al.[13c] was augmented with gradient-corrected functionals for electron exchange according to Becke[13d] and correlation according to Perdew[13e] in a self-consistent fashion. This gradient-corrected density functional is usually termed BP86 in the literature and was shown to be able to describe both energetic and structural aspects of organolanthanide compounds reliably.[14] The suitability of the BP86 functional for the reliable determination of the energy profiles for the various elementary processes in the organolanthanide-supported ROZP of methylenecycloalkanes has been substantiated (see Supporting Information), and this allows mechanistic conclusions having substantial predictive value to be drawn. Since all species investigated in this study show a large HOMO–LUMO gap, a spin-restricted formalism was used for all calculations.

For Sm we used the Stuttgart–Dresden quasirelativistic effective core potential (SDD) with the associated (7s6p5d)/[5s4p3d] valence basis set contracted according to a (31111/3111/311) scheme.[15] This ECP treats $[Kr]4d^{10}4f^5$ as a fixed core, whereas $5s^25p^66s^25d^16p^0$ shells are taken into account explicitly. All other elements were represented by Ahlrichs'

split-valence SV(P) basis set[16a] with polarization functions on heavy main group atoms, but not on hydrogen; that is, for carbon a 7s/4p/1d set contracted to (511/31/1) and for hydrogen a 4s set contracted to (31). The geometry optimization and the saddle-point search were carried out by utilizing analytical/numerical gradients/Hessians according to standard algorithms. No symmetry constraints were imposed in any case. This level of basis-set quality has been identified as a reliable tool for the assessment of structural parameters and vibrational frequencies.[17] The stationary points were identified exactly by the curvature of the potential-energy surface at these points corresponding to the eigenvalues of the Hessian. All reported transition states have exactly one negative Hessian eigenvalue, while all other stationary points exhibit exclusively positive eigenvalues. Each transition state was further confirmed by following its imaginary vibrational mode downhill on both sides to yield the reactant and product minima presented on the reaction profile for the individual steps. The many isomers that are possible for each of the investigated species were carefully explored. The reaction and activation enthalpies and free energies (ΔH, $\Delta H^{\neq}$ and ΔG, $\Delta G^{\neq}$ at 298 K and 1 atm) were evaluated according to standard textbook procedures[18] using computed harmonic frequencies. To obtain more accurate energy profiles, all key species were fully located by employing a more accurate basis set consisting of the aforementioned basis set for Sm and Ahlrichs' valence triple-ζ TZVP basis set[16b] with polarization functions on all other atoms, that is, for carbon a 11s/6p/1d set contracted to (62111/411/1) and for hydrogen a 5s/1p set contracted to (311/1).

To study the influence of nonspecific solute–solvent interactions[19] on the energy profile of individual elementary steps, the solvent was described as a homogeneous, isotropic, linear dielectric medium within the conductorlike screening model (COSMO) due to Klamt and Schüürmann[20] as implemented in Turbomole.[21] Environment effects were estimated for toluene (dielectric constant $\varepsilon = 2.378$ at 298 K),[22] one of the experimentally used solvents.[7c] Nonelectrostatic contributions to solvation were not considered. The solvation effects were included self-consistently in the calculations, and all key species were fully optimized with inclusion of solvation at the BP86/SDD-TZVP level. The optimized atomic COSMO radii ($r_H = 1.3$ Å, $r_C = 2.0$ Å)[23] were used in combination with the unoptimized radius of 2.22 Å for Sm. For each of the investigated elementary processes, both the structural and the energetic aspects were reproduced in great similarity by the gas-phase and COSMO approaches at the BP86/SDD-TZVP level, so that both computational methods (as well as the B3-LYP/SDD-TZVP method) can be considered as being equally competent for the investigation of the fine mechanistic details of the title reaction (see Supporting Information for more details).

Energetics (BP86/SDD-TZVP) on the ΔH(298 K) surface were reported as ΔE plus zero-point energy correction at 0 K plus thermal-motion corrections at 298 K plus solvation correction. The Gibbs free energies were obtained as $\Delta G_{298} = \Delta H_{298} - T\Delta S$ at 298 K and 1 atm. The $T\Delta S$ contribution of about 11–13 kcal mol^{-1} (under standard conditions) calculated for PhMCP coordination in the gas phase certainly does not reflect the real entropic cost for substrate association and dissociation under actual catalytic conditions.[7c] The difference in the reaction entropy for the $Cp_2LnR + PhMCP \rightarrow PhMCP\text{-}Cp_2LnR$ substrate uptake process taking place in the gas phase and condensed phase is mainly due to substrate solvation, since the solvation entropies of the Cp_2LnR starting material and the PhMCP-Cp_2LnR adduct can be regarded as being similar. The solvation entropy of ethylene, as a prototypic olefin, is about 16 eu in typical aromatic hydrocarbon solvents,[24] which can reasonably be adopted for methylenecycloalkanes as well. This reduces the entropic cost for substrate complexation by about 4.8 kcal mol^{-1} (298.15 K), that is, about two-thirds of the gas-phase value. This estimation agrees reasonably well with the findings of a recent theoretical study, which showed that for polar solvents the entropies in solution decrease to nearly half of the gas-phase value.[25] Therefore, the solvation entropy for substrate association and dissociation was approximated as being two-thirds of its gas-phase value, which the author considers to be a reliable estimate of the entropy contribution in the condensed phase. All the drawings were prepared by employing the program Struked.[26]

Results and Discussion

The theoretical mechanistic investigation of the chain-initiation process starts with a careful step-by-step exploration of the elementary processes outlined in Scheme 1. This examination is aimed at elucidating the crucial features of each of the individual steps and at proposing the most feasible of the various conceivable pathways. From the detailed insight obtained for the critical elementary steps, a free-energy profile comprised of thermodynamic and kinetic aspects for the respective favorable pathways is presented and the implications regarding the operative mechanism and the regioselectivity of the process are elucidated.

Exploration of crucial elementary steps

Insertion of the exo-methylene group into the Sm–H bond of 1: As mentioned in the introduction, for the insertion of the *exo*-methylene group of PhMCP into the Sm–H bond of **1** in 1,2 or 2,1 fashion, two different pathways are conceivable in each case. They are distinguished by the relative arrangement of the phenyl group towards the metal center, with the Sm–H and secondary C^3–Ph bonds in *syn* and *anti* orientation, respectively (Scheme 2). For systems that are moderately encumbered sterically, the species involved along the *syn* pathway can be envisioned to benefit from an effective phenyl–Sm interaction, as indicated in Scheme 2,[27] as opposed to the *anti* pathway, where this cannot be accomplished.

The key species participating along the two alternative pathways are labeled by an additional **a** and **s** for the *anti* and *syn* pathways, respectively, and are shown in Figure 1 for the 1,2-insertion process, while the 2,1-insertion analogues are included in the Supporting Information (see Figure S1). The complete energetics are collected in Table 1. As revealed by Figure 1 (S1), uptake of the substrate in **1** leads first to the encounter complex **1**-PhMCP, in which PhMCP is coordinated in such a way that the C=C bond and the cyclopropane ring are coplanar and perpendicular, respectively, to the Sm–H bond. Accordingly no further reorganizations are required for *exo*-methylene C=C insertion into the Sm–H bond to occur. A four-membered transition-state structure with a square-planar *cis* arrangement of the Sm–H bond and the exocyclic C=C bond is encountered along the minimum-energy pathway for both the 1,2- and 2,1-insertion steps and occurs at a distance of about 2.2–2.5 Å of the newly formed C–H bond. Decay of the TS gives rise first to product species (**2a**, **2s** and **3a**, **3s** for 1,2- and 2,1-insertion, respectively) with a perpendicularly oriented cyclopropyl ring, which afterwards relax readily into thermodynamically more favorable isomers with an in-plane-rotated ring (e.g., the **2a′**, **2a″**, **2s′**, **2s″** 1,2-insertion species; see below).

However, the minimum-energy pathway reported here, which bears great similarity to olefin insertion into M–C and M–H bonds,[28] is in sharp contrast to that found in a previous computational investigation of MCP insertion into

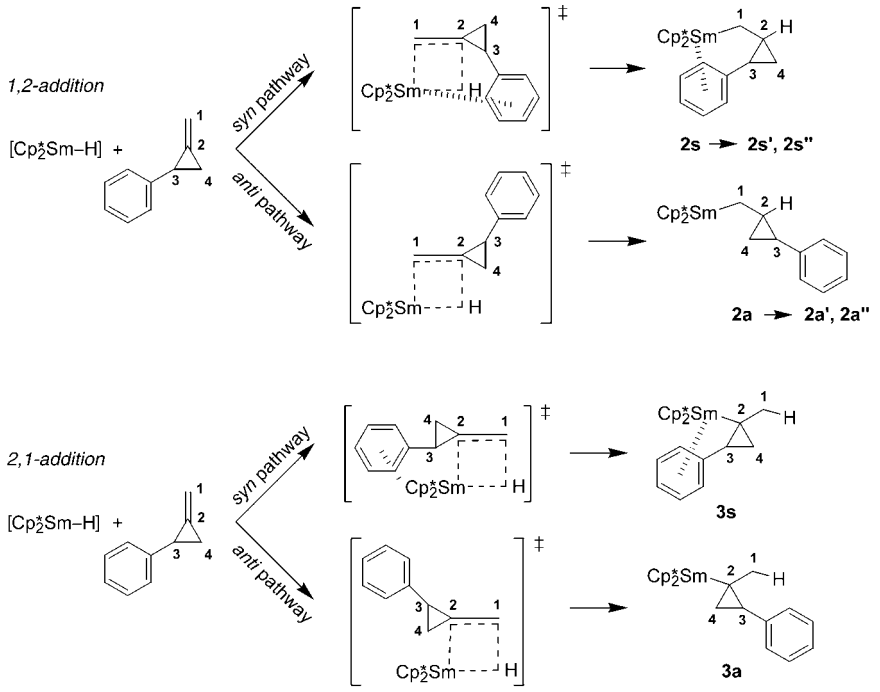

Scheme 2. The two alternative pathways for insertion of the exocyclic C=C bond of PhMCP into the Sm–H bond of **1** in 1,2- or 2,1-fashion.

the Ln–H bond of Cp_2LnH complexes (Ln = La, Lu).[11a,b] A tetrahedral transition-state structure that is associated with a huge barrier of 31.9 and 39.9 kcal mol^{-1} ($\Delta E^{\neq}$), respectively, was reported.[11b] The rather uncommon TS geometry and the predicted unfavorable kinetics, which contradict our findings (vide infra), may argue against the adequate representation of both structural and energetic aspects in these studies.[11c]

Inspection of the *syn* 1,2-insertion pathway does not provide any indication of effective phenyl–Sm coordination until the process reaches **2s** (see Figure 1), owing to unfavorable steric interactions of the phenyl group with the Cp_2Sm backbone and/or the *cis* Sm–H bond. Therefore, the aryl substituent is not likely to accelerate the process kinetically through a stabilizing interaction with the electrophilic metal center, but it affects the thermodynamics. The subsequent relaxation to thermodynamically more stable isomers through facile rotation of the cyclopropyl ring from a perpendicular (e.g., as in **2s**) to an in-plane orientation can occur in two directions to give rise to species in which the phenyl group points away (denoted by a single prime, for example, **2s**′) or towards (denoted by a double prime, for example, **2s**″) the metal center. Species **2s**″, **2a**″ are stabilized relative to **2s**′, **2a**′, respectively, by effective η^2 coordination of the phenyl group that is of comparable strength in both **2s**″ and **2a**″. The alternative 2,1-insertion step exhibits a similar characteristic. Due to the absence of interactions with the Sm–H moiety in this case, the phenyl group displays a larger tendency for interaction with the lanthanide along the *syn* pathway in both the encounter complex and the TS compared to the analogues of the *syn* 1,2-pathway. The intensified phenyl–Sm coordination, however, comes at the expense of the methylene–Sm bond strength (see Figure S1 in the Supporting Information), which acts as a counterbalancing factor. Of the two kinetic product species **3a** and **3s**, which do not undergo further rotations of the cyclopropyl moiety, **3s** is clearly seen to be stabilized substantially by a close phenyl–Sm interaction. Overall, the kinetics of the insertion step, proceeding either in 1,2 or in 2,1 fashion, is indicated to not benefit from stabilizing coordinative interactions between the arene ring and the electrophilic lanthanide center.

The energy profile summarized in Table 1 reveals that both the 1,2- and 2,1-insertion steps are facile and irreversible processes which are driven by a strong thermodynamic force exceeding −16 kcal mol^{-1} (ΔG). The readily formed encounter complex (i.e., in a barrierless process) and also the transition states for the various pathways all lie below the energy of the entrance channel of the **1**+PhMCP process at the enthalpic surface. The entropic contributions associated with this bimolecular step shift the free-energy profile above the entrance channel and result in small activation free energies of only 6.2–7.2 kcal mol^{-1} for the favorable *anti* pathways for 1,2- and 2,1-insertion (see Table 1).

The structural aspects of the individual pathways analyzed before are paralleled in the computed energetics. Considering the 1,2-insertion step first, the *anti* pathway is predicted to be preferred kinetically relative to the *syn* pathway by a barrier that is 3.5 kcal mol^{-1} ($\Delta\Delta G^{\neq}$) lower, because unfavorable steric interaction between the arene ring and the catalyst backbone are not present along the *anti* pathway. The *syn* pathway is driven by a slightly larger thermodynamic force, which, however, is of little relevance for the strongly exergonic and thus irreversible insertion step. The insertion proceeding in 2,1 fashion exhibits similar energetics, with kinetics almost identical to the 1,2-insertion step. In analogy to the aforementioned argumentation, the *anti* pathway is most feasible kinetically ($\Delta\Delta G^{\neq}$ = 2.1 kcal mol^{-1}), while the extra stabilization of **3s** by η^2-phenyl coordination results in a larger heat of reaction for the *syn* pathway.

Overall, the phenyl substituent discriminates between the two alternative pathways for insertion to proceed in either 1,2 or 2,1 fashion. In both cases the *anti* pathway is predicted as being favorable kinetically, owing to the absence of

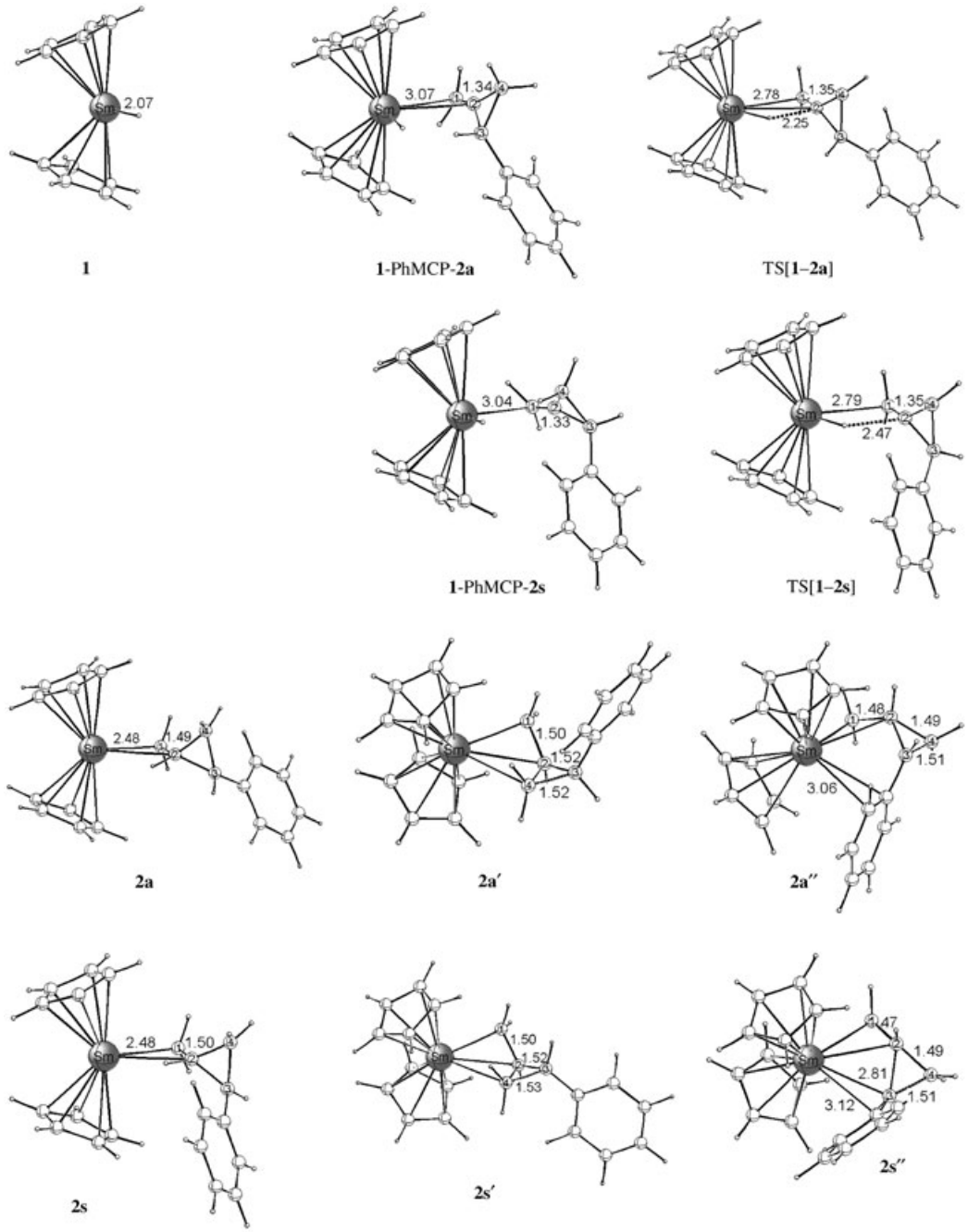

Figure 1. Selected geometric parameters [Å] of the optimized structures of key species for the alternative *anti* and *syn* pathways for 1,2-insertion of the exocyclic C=C bond of PhMCP into the Sm−H bond of **1**. The cutoff for drawing Ln−C bonds was arbitrarily set to 3.1 Å.

unfavorable steric interactions between the phenyl group and the catalyst backbone.

β-Alkyl shift-based ring opening: Decomposition of the cyclopropyl ring in the insertion products is the step that is encountered next in the course of the reaction (see Scheme 1); its complete energetics are compiled in Table 2. The minimum-energy path for ring opening in mechanistic cycle **I** (Scheme 1), proceeding by cleavage of either of the two proximal bonds, is characterized by precursor species in which the cyclopropyl ring is in coplanar orientation (relative to the Sm-C^1-C^2 moiety), and the respective bond to be broken is *cis*-arranged, pointing towards the metal atom. Thus, the thermodynamically prevalent isomers of the insertion product represent the direct precursor for cycle degradation. Species **2a′**, **2s′** are the precursors for the pathway involving proximal-bond cleavage (i.e., C^2–C^4 bond scission) where the phenyl group is remote from the metal center, while the alternative pathway (i.e., C^2–C^3 bond scission) with an adjacent phenyl group starts from **2a″** and **2s″**

Table 1. Enthalpies and free energies of activation and reaction for insertion of the exocyclic C=C bond of PhMCP into the Sm–H bond of catalyst **1** proceeding in 1,2- (**1**+PhMCP→**2a**/**2s**) or 2,1-fashion (**1** + PhMCP→**3a**/**3 s**).[a–c]

PhMCP insertion path	PhMCP insertion pathway: PhMCP π complex	TS	product[d]
1,2-insertion			
anti pathway	−4.5/*4.0* **1**-PhMCP-**2a**	−2.8/*6.2*	−23.2/−*14.1* **2a**
			−27.1/−*17.8* **2a′**
			−29.2/−*19.6* **2a″**
syn pathway	−2.3/*6.2* **1**-PhMCP-**2s**	0.7/*9.7*	−23.9/−*14.9* **2s**
			−29.3/−*20.1* **2s′**
			−30.7/−*21.2* **2s″**
2,1-insertion			
anti pathway	−3.0/*5.5* **1**-PhMCP-**3a**	−0.9/*7.2*	−24.8/−*15.9* **3a**
syn pathway	−0.8/*7.9* **1**-PhMCP-**3 s**	−0.7/*9.3*	−30.0/−*21.0* **3 s**

[a] This process is classified according to the kind of PhMCP insertion involved (see Scheme 2). [b] Total barriers and reaction energies are relative to **1**+PhMCP. [c] Activation enthalpies and free energies (ΔH^{+}/ΔG^{+}) and reaction enthalpies and free energies (ΔH/ΔG) are given in kilocalories per mole; numbers in italic type are the Gibbs free energies. [d] See text for description of the various isomers.

Table 2. Enthalpies and free energies of activation and reaction for β-alkyl shift-based ring opening occurring in the mechanistic cycles **I** (**2a′**/**2s′**→**4r′** and **2a″**/**2s″**→**4j′**) and **II** (**3a**→**5a′** and **3 s**→**5 s′**).[a–c]

PhMCP insertion path	Ring-opening pathway: precursor[d]	TS	product
1,2-insertion		proximal C^2–C^4 bond	
anti pathway	3.6/*3.4* **2a′**	6.2/*6.3*	2.8/*1.5* **4r**//1.3/*0.0* **4r′**
syn pathway	1.4/*1.1* **2s′**	4.4/*4.5*	−1.1/-*2.4* **4r**//1.1/−*0.2* **4r′**
1,2-insertion		proximal C^2–C^3 bond	
anti pathway	1.5/*1.6* **2a″**	1.6/*1.7*	−9.1/−*9.5* **4j**//−8.7/−*10.3* **4j′**
syn pathway	0.0/*0.0* **2s″**	0.3/*0.5*	−8.7/−*9.0* **4j**//−8.8/−*10.3* **4j′**
2,1-insertion		distal C^3–C^4 bond[e]	
anti pathway	0.0/*0.0* **3a**	35.7/*35.3* $\eta^1(C^3)$-allylic	−20.2/−*20.5* **5a**
		30.7/*30.9* η^3-allylic	−28.2/−*28.1* **5a′**
syn pathway	0.0/*0.0* **3 s**	27.2/*27.3* $\eta^1(C^3)$-allylic	−15.0/−*15.5* **5 s**
		27.9/*28.5* η^3-allylic	−23.0/−*23.1* **5 s′**

[a] This process is classified according to the type of bond cleaved in the cyclopropyl ring. The relationship to the prior insertion step is explicitly given. [b] Total barriers and reaction energies are relative to the prevalent insertion product isomers of the 1,2-initiated (i.e., **2s″**) and relative to **3a** and **3 s** for 2,1-initiated cycles. [c] Activation enthalpies and free energies (ΔH^{+}/ΔG^{+}) and reaction enthalpies and free energies (ΔH/ΔG) are given in kilocalories per mole; numbers in italic type are Gibbs free energies. [d] See text for description of the various isomers. [e] Two different types of located transition state having an $\eta^1(C^3)$- or η^3-allylic structure are reported.

(Scheme 3). This affords ring-opened product species **4r**, **4r′** and **4j**, **4j′**, respectively, (labeled by an additional **r** or **j** to indicate the remote or adjacent phenyl substituent) of different regiochemistry. The two routes (e.g., **2a′**→**4r** and **2s′**→**4r**) for each of the pathways are characterized by structural and energetic features that are almost identical. Thus, the key species are presented for only one of the routes for each pathway (Figure 2), while the analogues are included in the Supporting Information (Figure S2).

Following the minimum-energy path commencing from **2a′**/**2s′** and **2a″**/**2s″** does not reveal further reorganizations to be necessary until the transition state is reached. Thus, ring opening takes place in a smooth fashion through elongation of the proximal C^2–C^4 and C^2–C^3 bonds, respectively (see Figure 2). By contrast to the insertion step, the adjacent phenyl group clearly acts to support ring opening along **2a″**/**2s″**→**4j** (C^2–C^3 bond cleavage) through a stabilizing interaction with the electrophilic Sm center, which is maintained during the whole process. The assistance provided by the phenyl group is also reflected in the located transition-state structures for the two pathways. The precursor-like transition state bears an η^2-phenyl moiety and has a length of the vanishing C^2–C^3 bond of 1.68 Å (only 0.02 Å longer than in the precursor species, Figure 2) is encountered along the **2a″**/**2s″**→**4j** pathway, that is, a highly facile transformation. On the other hand, the transition state for the **2a′**/**2s′**→**4r** pathway occurs at a distance of 1.92 Å for the C^2–C^4 bond to be cleaved, which can be regarded as being product-like. The transition states decay first into the η^2,η^1-alkenyl Sm species **4r** and **4j** for the processes that starts from **2a′**/**2s′** and **2a″**/**2s″**, respectively. Species **4j** clearly benefits from η^3-benzylic coordination of the phenyl group,[29] that is, the **2a″**/**2s″**→**4j** pathway is also favored kinetically by a larger thermodynamic force when compared to the alternative **2a′**/**2s′**→**4r** pathway, which is not assisted by the coordinating phenyl group. The initially formed ring-opened species **4r** and **4j** readily undergo transformation into isomers **4r′** and **4j′** by displacing the double bond from the metal center though a kinetically facile rotation around the C^3–C^4 bond, which comes to the advantage of a weak phenyl–Sm interaction and an amplified η^3-benzylic interaction, respectively (Figure 2).

The reaction path for ring opening of the MCP 1,2-insertion product reported previously[11a,b] is distinctly different from the smooth process described thus far. This process was found to be kinetically expensive (ΔE^{+} = 28.4 and 32.6 kcal mol^{-1} for the La- and Lu-mediated reactions, respectively),[11b] which is in sharp contrast to our results (vide infra) and is connected with a transition state that constitutes ring opening with simultaneous switching of an H atom between the C^2 and C^4 carbon atoms. The located transition-state structure is certainly not likely to be encountered along the minimum-energy path of the process, which does not require the shift of an H atom. This amplifies the doubts about the reliability of the previous studies,[11a,b] as already argued above. Accordingly, this leads us to conclude that the mechanistic conclusions drawn there,[11a,b] which are

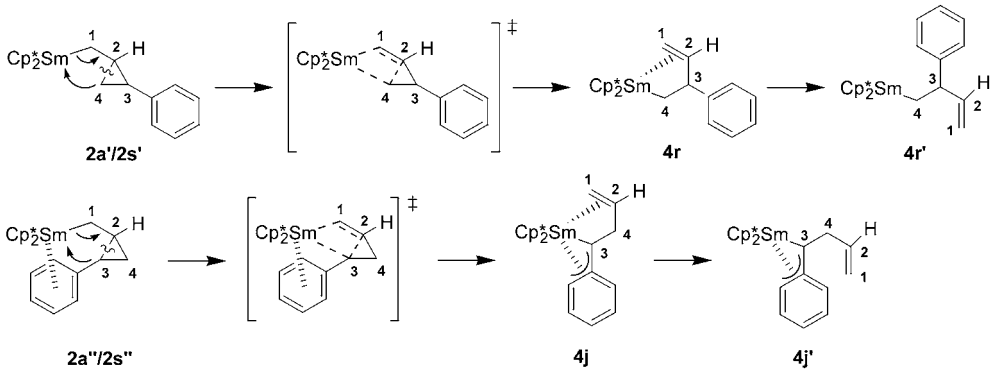

Scheme 3. The two alternative pathways for β-alkyl shift-based ring opening by cleavage of a proximal bond of the cyclopropyl ring along cycle **I**.

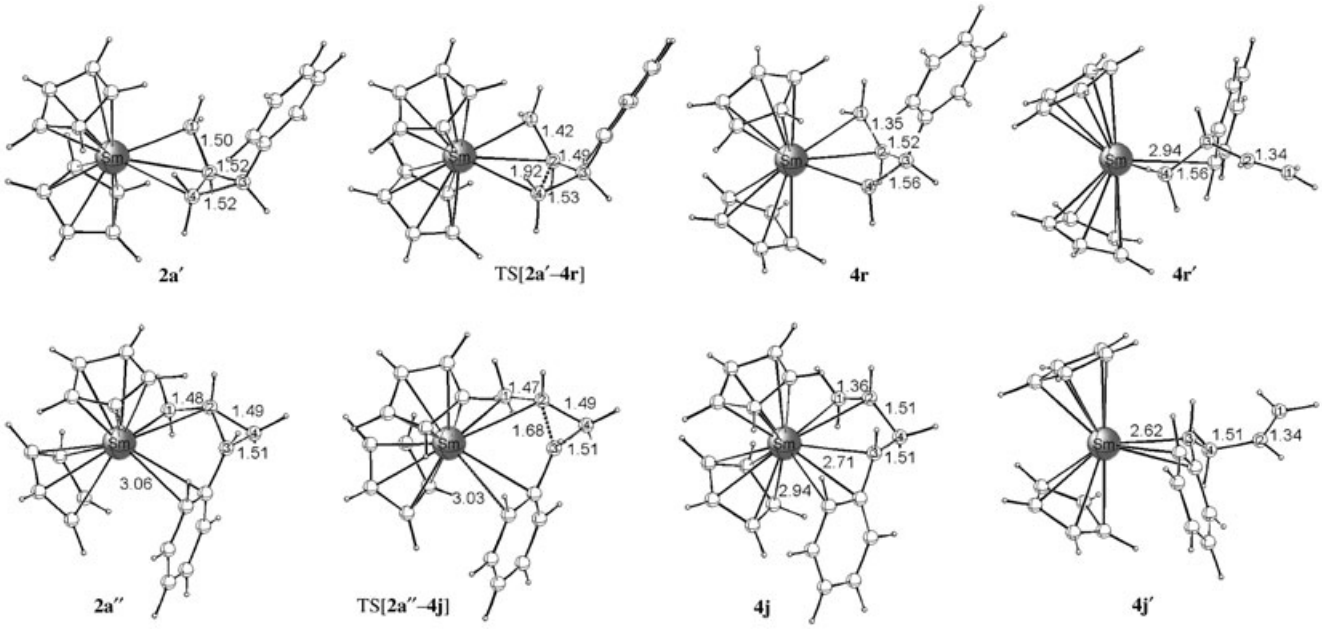

Figure 2. Selected geometric parameters [Å] of the optimized structures of key species for ring opening of the 1,2-insertion product (cycle **I**) by cleavage of a proximal bond of the cyclopropyl ring occurring through alternative pathways with the phenyl substituent located remote from (top) or adjacent to (bottom) the metal center. The cutoff for drawing Ln–C bonds was arbitrarily set to 3.1 Å.

based on located transition-state structures that seem entirely implausible, do not have any relevance.[11c]

Ring opening by cleavage of one of the proximal bonds is predicted to be highly facile kinetically (see Table 2). In parallel to the above discussed structural features, the **2a**″/**2s**″→**4j** pathway is the preferred one among the two regioisomeric pathways, on both kinetic and thermodynamic grounds, owing to stabilizing coordinative phenyl–Sm interactions. An activation free energy of only about 0.5–1.7 kcal mol^{-1} must be overcome along this pathway, which yields **4j** and **4j**′, respectively, in an exergonic process that is driven by a thermodynamic force of −(9–10) kcal mol^{-1}. This indicates that ring opening along the favorable **2a**″/**2s**″→**4j** pathway is an irreversible process that occurs instantaneously. The ring-opened regioisomers **4r**, **4r**′ are, on the other hand, formed in an essentially thermoneutral, reversible process that has a barrier of 4.5–6.3 kcal mol^{-1} ($\Delta G^{\neq}$). Thus, similar to the findings for the insertion step (see above), the phenyl group discriminates between the two possible pathways for β-alkyl shift-based ring opening (see Scheme 3). In contrast to the insertion step, however, decomposition of the cyclopropyl ring is distinctly facilitated kinetically and also thermodynamically by the coordinative interaction of the electrophilic lanthanide center with the π system of the adjacent phenyl ring.[27]

In cycle **II** (Scheme 1) regioisomeric products **3a** and **3s** are precursors for the subsequent ring-opening process. The most feasible route for degradation of the cyclopropyl ring proceeds through cleavage of the distal C^3–C^4 bond. The two possible pathways, in which the phenyl group has an *anti* (**3a**→**5a**/**5a**′) or a *syn* (**3s**→**5 s**/**5 s**′) disposition with regard to the Sm–C^2 bond, lead to 1-phenyl,2-methallyl–Sm product isomers[10] having identical regiochemistry (Scheme 4), which is in contrast to the situation for mechanistic cycle **I** (vide supra).

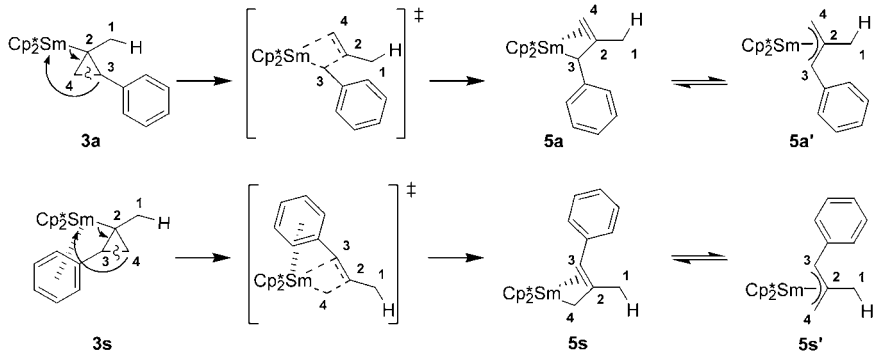

Scheme 4. The two alternative pathways for β-alkyl shift-based ring opening by cleavage of the distal bond of the cyclopropyl ring along cycle **II**.

A detailed survey of several conceivable ways to generate the allyl–Sm product species revealed that this can occur through transition states with an elongated C^3–C^4 bond that are characterized by an already preformed allylic moiety adopting $\eta^1(C^3)$-σ (TS[**3a**-**5a**] and TS[**3s**-**5s**]) or η^3-π modes (TS[**3a**-**5a**′] and TS[**3s**-**5s**′]) of allyl coordination to Sm. The corresponding key species for the two pathways with *anti*- and *syn*-disposed phenyl group (see

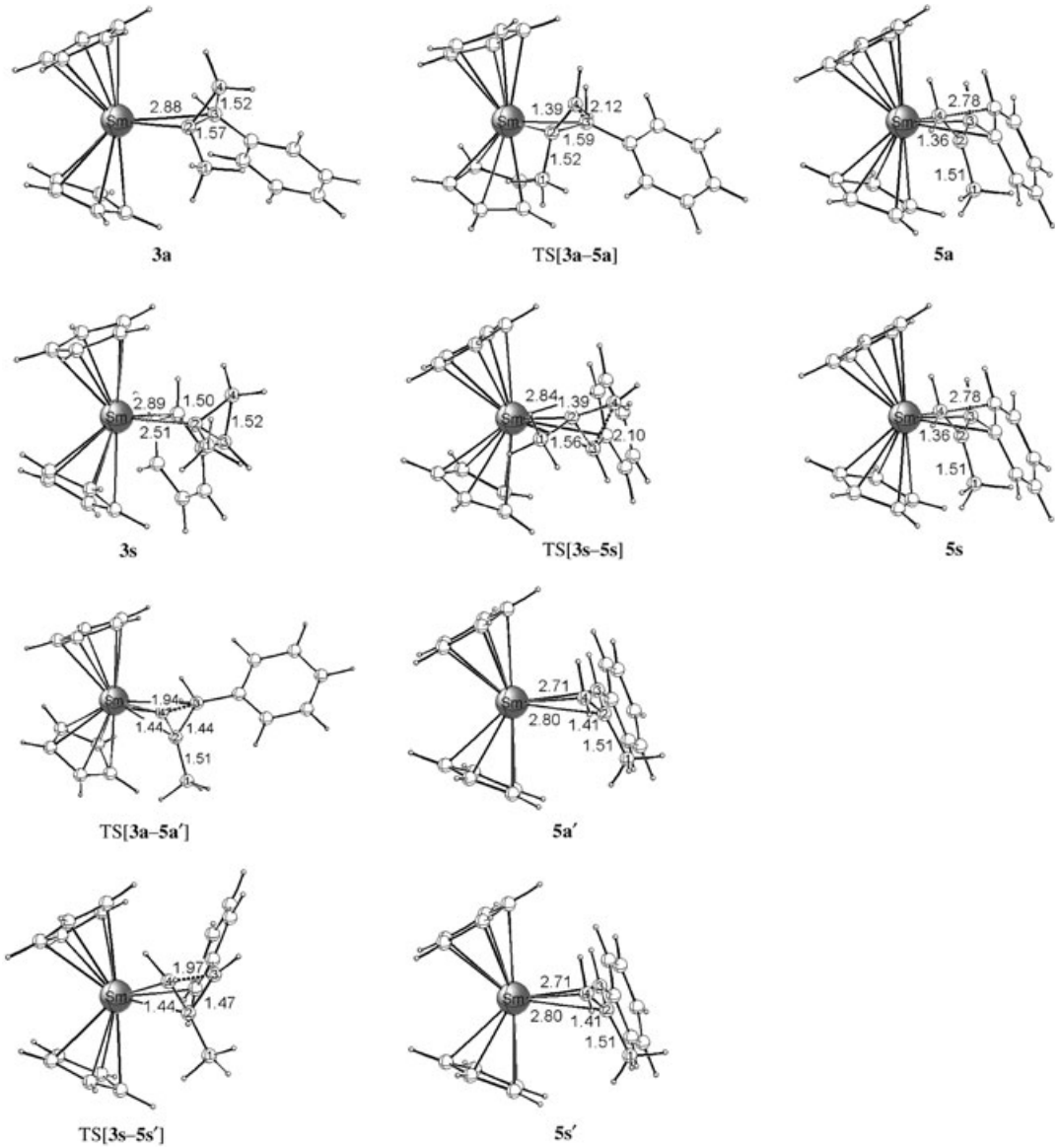

Figure 3. Selected geometric parameters [Å] of the optimized structures of key species for ring opening of the 2,1-insertion product (cycle **II**) by cleavage of the distal cyclopropyl bond occurring through alternative pathways with the phenyl substituent in an *anti* or a *syn* disposition with respect to the Sm–C^2 bond. The cutoff for drawing Ln–C bonds was arbitrarily set to 3.1 Å.

Scheme 4) are displayed in Figure 3, which shows that the **3s**→**5s**/**5s′** pathway takes advantage of the attainable phenyl–Sm interaction. This is most pronounced for TS[**3s**-**5s**] (and **5s**), in which the phenyl substituent compensates the partial coordinative unsaturation caused by the $\eta^1(C^3)$-σ-allylic moiety through effective η^3-benzylic coordination, but is also seen in TS[**3s**-**5s′**] with a preformed η^3-allylic moiety. The absence of this stabilizing interaction along **3a**→**5a**/**5a′** renders this pathway distinctly more difficult kinetically (vide infra). Focusing on the more feasible of the two pathways, TS[**3s**-**5s**] emerges at a distance of 2.1 Å for the vanishing C^3–C^4 distal bond and decay into the $\eta^1(C^3)$-σ-allylic product species **5s**, while TS[**3s**-**5s′**] appears somewhat earlier (1.97 Å) and leads to the *syn*-η^3-allyl form **5s′**. Interconversion between the **5s** and **5s′** forms, with the latter thermodynamically prevalent (see Table 2), is likely to be a facile process.[30]

Similar to the findings for cyclopropyl ring opening of 1,2-insertion products, the **3s**→**5s**/**5s′** pathway, which benefits from the phenyl–Sm interaction, is predicted to be kinetically more feasible than the **3a**→**5a**/**5a′** pathway. Both of these afford products of identical regiochemistry in an irreversible process that is driven by a strong thermodynamic force with an exergonicity of $-23.1\ \mathrm{kcal\,mol^{-1}}$ (Table 2). Interestingly, the phenyl substituent compensates the coordinative deficiencies in TS[**3s**-**5s**] efficiently, so that very similar activation barriers of 27.3–28.5 $\mathrm{kcal\,mol^{-1}}$ ($\Delta G^{\neq}$) are associated with the ring-opening process passing through TS[**3s**-**5s**] and TS[**3s**-**5s′**]. Higher barriers are predicted for the **3a**→**5a**/**5a′** pathway with a remote phenyl group, and TS[**3a**-**5a**] was found to be exceptionally high in energy ($\Delta G^{\neq} = 35.3$ kcal $\mathrm{mol^{-1}}$) due to the lack of coordinative stabilization.

Overall, cleavage of the distal bond of the cyclopropyl ring is predicted to be significantly more difficult kinetically than proximal bond scission occurring along cycle **I**, which starts with 1,2 insertion (see below)

β-H elimination to afford the ring-opened phenyl-1,3-butadiene isomers: After completion of chain initiation in cycle **I** with formation of **4r**/**4r′** and **4j**/**4j′**, respectively, the reaction can proceed further by PhMCP enchainment in a ring-opened fashion or, as a conceivable alternative, by β-H elimination to afford phenyl-1,3-butadienes as ring-opened PhMCP isomers. Among the various routes that have been surveyed computationally, the most feasible starts from **4r′** and **4j′**. The process with **4r** and **4j** as precursor is accompanied by displacement of the olefinic subunit from the immediate proximity of the metal center and thus approaches the corresponding **4r′** and **4j′** isomers in the vicinity of the transition state. β-H elimination along the alternative pathways commencing from the **4r′** and **4j′** regioisomers, in which the phenyl substituent is located remote from or adjacent to the metal center, gives rise to the 2-phenyl- and 1-phenyl-1,3-butadiene hydride Sm species **6r** and **6j**, respectively (Scheme 5).

The transition state TS[**4r′**-**6r**] shows, not unexpectedly, great similarity to the transition state for 2,1-insertion (see above). It exhibits a hydrido–Sm bond that seems to be already almost fully established, a substantially elongated C^3–H bond, and a preformed η^2-coordinated butadiene moiety (Figure 4). The phenyl group that is weakly coordinated in **4r′** becomes displaced from the metal center during the elimination process. The decay of the productlike TS[**4r′**-**6r**] leads to the η^2-(2-phenylbutadiene)–Sm hydride product **6r**, which resembles the PhMCP encounter complex for the 2,1-insertion step. The formal resemblance between the **4r′**→**6r** and **1**+PhMCP→**3a** processes is also paralleled in the energetics (Table 3). The β-H elimination is an endergonic process ($\Delta G = 8.7\ \mathrm{kcal\,mol^{-1}}$) that is associated with an activation barrier of 14.3 $\mathrm{kcal\,mol^{-1}}$ ($\Delta G^{\neq}$) and is thus nearly the inverse of the insertion step.

The process occurring along the alternative **4j′**→**6j** pathway is also accompanied by the displacement of the phenyl group from the immediate proximity of the metal atom (Figure 4). Commencing from the precursor with an η^3-benzylic substituent, TS[**4j′**-**6j**] is characterized by a significantly diminished phenyl–Sm interaction and has structural features that are comparable with those of TS[**4r′**-**6r**]. A similar, but slightly higher, barrier ($\Delta G^{\neq} = 16.4\ \mathrm{kcal\,mol^{-1}}$, see Table 3) must be overcome along **4j′**→**6j** to give rise to the η^2-(1-phenylbutadiene)–Sm hydride product in a process that has a larger endergonicity ($\Delta G = 14.0\ \mathrm{kcal\,mol^{-1}}$) than the **4r′**→**6r** pathway. This increased thermodynamic disfavor is understandable from the aforementioned fact that the re-

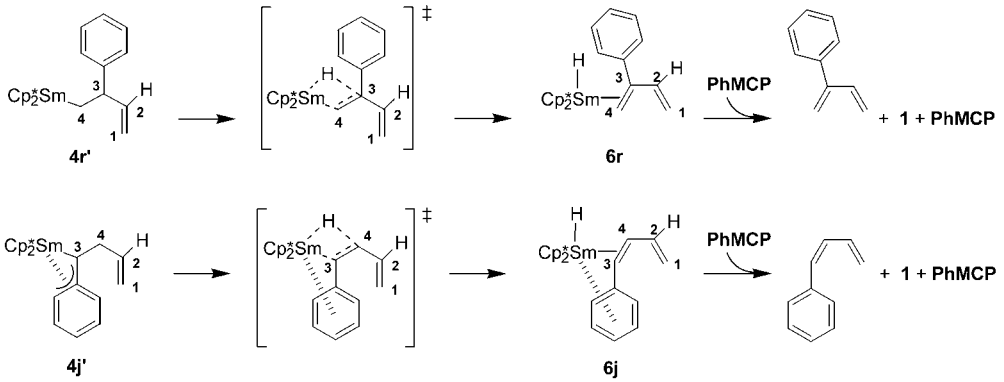

Scheme 5. The two alternative pathways for β-H elimination to afford phenylbutadienes as ring-opened PhMCP isomers along cycle **I**.

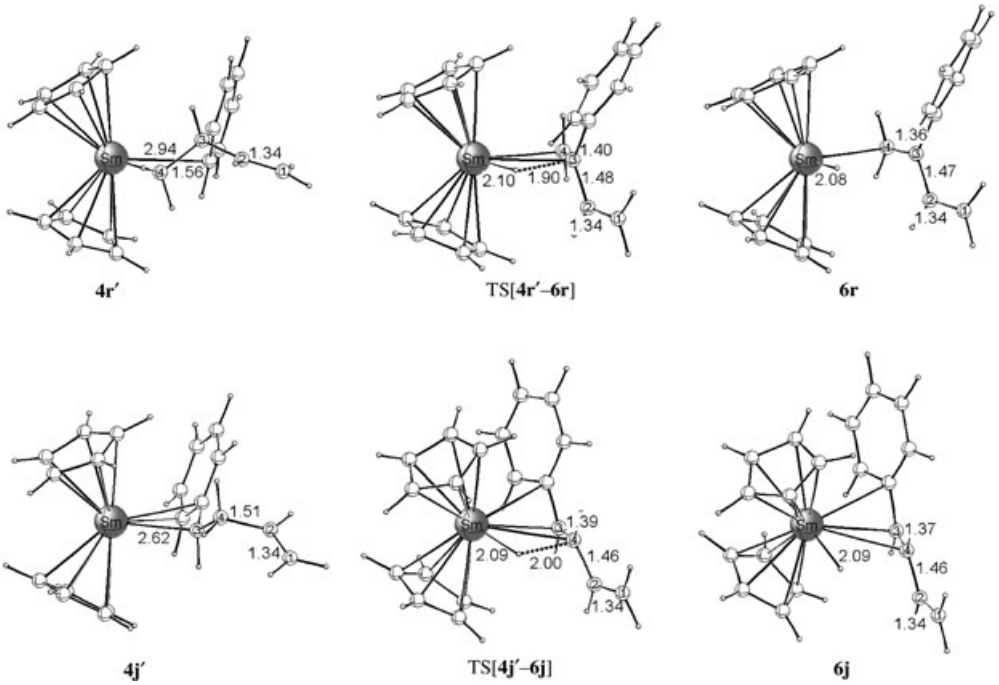

Figure 4. Selected geometric parameters [Å] of optimized structures of key species for β-H elimination in the ring-opened species along cycle **I** occurring through alternative pathways with the phenyl substituent located remote from (top) or adjacent to (bottom) the metal center. The cutoff for drawing Ln–C bonds was arbitrarily set to 3.1 Å.

Table 3. Enthalpies and free energies of activation and reaction for β-H elimination along **4r′**→**6r** and **4j′**→**6j** to afford phenylbutadienes as ring-opened PhMCP isomers.[a–c]

PhMCP insertion path	β-H elimination pathway precursor	TS	product
1,2-insertion			2-phenyl-butadiene **6r**
anti pathway	0.2/*0.2* **4r′**	14.2/*14.5*	9.9/*8.9*
syn pathway	0.0/*0.0* **4r′**	14.3/*14.6*	9.9/*8.9*
1,2-insertion			1-phenyl-butadiene **6j**
anti pathway	0.1/*0.0* **4j′**	15.6/*16.4*	14.5/*14.0*
syn pathway	0.0/*0.0* **4j′**	15.6/*16.5*	14.5/*14.0*

[a] This process is classified according to the stereoisomer of the precursor involved (see Scheme 5). The relationship to the prior insertion step is explicitly given. [b] Total barriers and reaction energies are relative to the precursors **4r′** and **4j′**, respectively. [c] Activation enthalpies and free energies ($\Delta H^{\neq}/\Delta G^{\neq}$) and reaction enthalpies and free energies ($\Delta H/\Delta G$) are given in kilocalories per mole; numbers in italic type are Gibbs free energies.

organization of phenyl–Sm coordination is more pronounced here.

The very similar kinetics ($\Delta\Delta G^{\neq} = 2.1$ kcal mol^{-1}, Table 3) predicted for the two alternative pathways indicates that the two 1-phenyl- and 2-phenylbutadiene regioisomers should be generated in comparable amounts as possible products of Sm-mediated PhMCP ring-opening polymerization, provided that the corresponding precursor species **4r′** and **4j′** occur in appreciable concentrations (see below). The phenylbutadienes are liberated from **6r** and **6j** through a subsequent substitution with PhMCP in slightly endergonic and exergonic processes ($\Delta G = 0.4$ and -2.4 kcal mol^{-1}, respectively) which regenerate the encounter complex **1**-PhMCP.

Catalytic reaction course of the chain-initiating process

Gibbs free-energy profile: On the basis of the careful computational exploration of the crucial elementary steps of the tentative course of the catalytic reaction (Scheme 1) reported above, the Gibbs free-energy profile (Scheme 6) is presented. It comprises thermodynamic and kinetic aspects of the two mechanistic cycles for [{Cp^*_2SmH}$_2$]-catalyzed chain initiation of ROZP of PhMCP. With this profile in hand, we can now elucidate the factors that are effective in discriminating between the alternative mechanisms and between the product regioisomers of chain initiation and substrate isomerization reactions, both occurring in a ring-opened fashion.

Factors governing the operative mechanism and the regioselectivity: The first insertion step is a facile and irreversible process that is driven by a strong thermodynamic force. For both the regioisomeric 1,2- and 2,1-insertion routes the *anti* pathway, in which the phenyl substituent is in remote location, is predicted to be kinetically favorable relative to the *syn* pathway ($\Delta\Delta G^{\neq} = 3.5$ and 2.1 kcal mol^{-1} for 1,2- and 2,1-insertion, respectively), owing to steric factors. Almost identical activation free energies are associated with the most feasible *anti* pathway for insertion proceeding in 1,2- ($\Delta G^{\neq} = 6.2$ kcal mol^{-1}) and 2,1-fashion ($\Delta G^{\neq} = 7.2$ kcal mol^{-1}),[31] and this indicates comparable probability

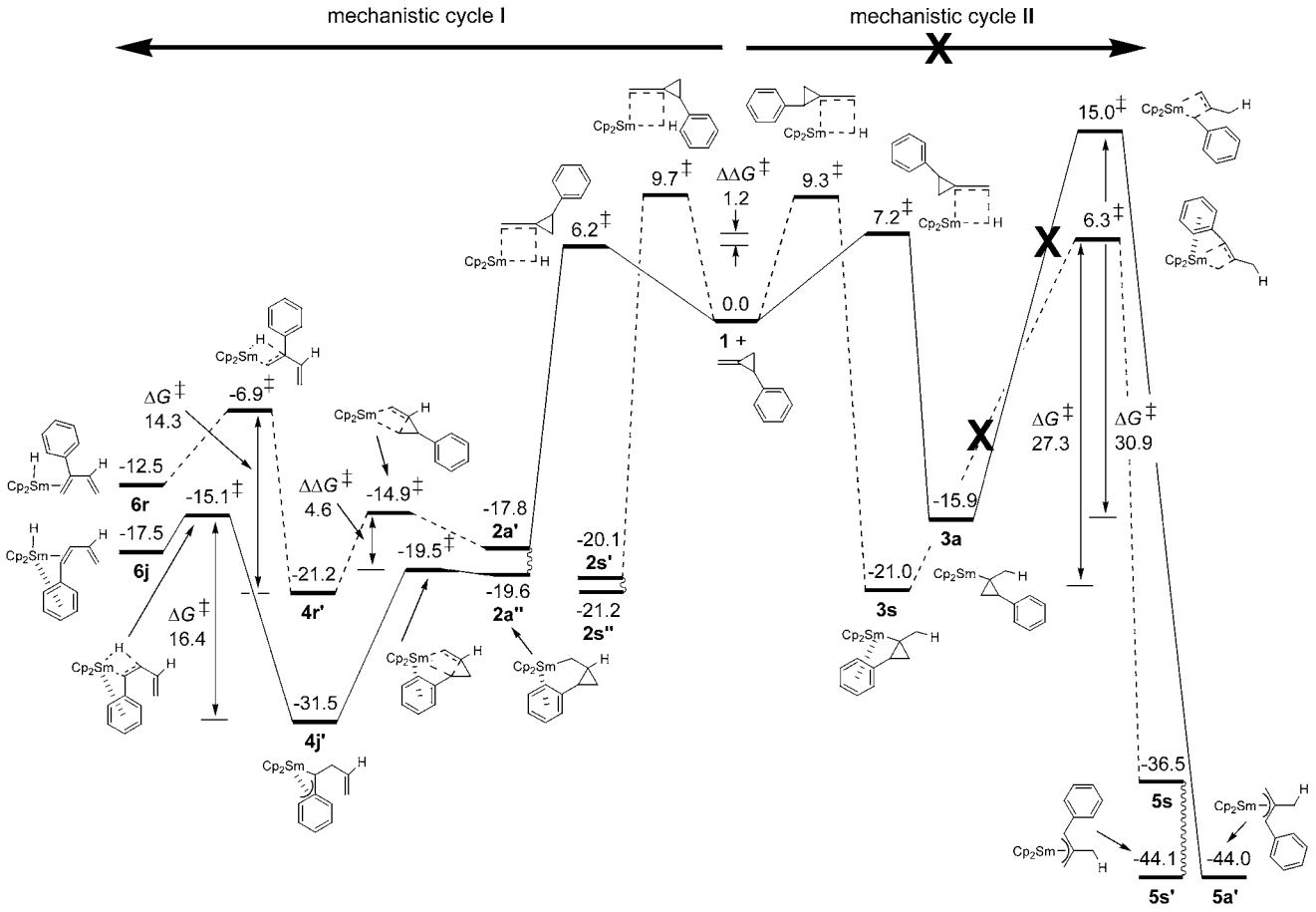

Scheme 6. Condensed Gibbs free-energy profile [kcal mol^{-1}] of ring-opened chain initiation and substrate isomerization in the organolanthanide-mediated polymerization of 2-PhMCP by model catalyst [Cp_2SmH]. The most feasible pathways for both mechanisms are represented by solid lines, and alternative pathways by dashed lines.

for both processes. This leads to the conclusion that insertion of the exocyclic C=C bond into the Sm–H bond does not proceed regioselectively. Accordingly, the first insertion step does not discriminate between the two conceivable mechanisms (see cycles **I**, **II** in Scheme 1) for chain initiation. Species **2a**′, **2a**″, and **3a** are the predominantly formed products of the two regioisomeric insertion routes. The predicted low barriers, which indicate the kinetically disfavored *syn* pathways ($\Delta G^{\ddagger}=9.3$–9.7 kcal mol^{-1}) to be viable as well, suggest that these pathways may also be accessible under catalytic reaction conditions,[7c] giving rise to **2s**, **2s**″, and **3s**, respectively, as possible products, albeit with distinctly smaller populations. Note that this scenario does not affect the further mechanistic conclusions.

The prevalent 1,2-insertion product species **2a**′, **2a**″, both of which are in equilibrium (see above), readily undergo subsequent ring opening ($\Delta G^{\ddagger}_{tot}=0.1$–$4.7$ kcal mol^{-1} relative to the most stable species **2a**″). By contrast, opening of the cyclopropyl ring commencing from **3a** is associated with a prohibitively large barrier of 30.9 kcal mol^{-1} ($\Delta G^{\ddagger}$), which is of similar magnitude but slightly smaller ($\Delta G^{\ddagger}=27.3$ kcal mol^{-1}) for the **3s**→**5s**′ pathway. As a consequence 1) the mechanistic cycle that starts with 1,2-insertion (see cycle **I** in Scheme 1) is almost exclusively entered and is thus operative in the chain-initiation process of [{Cp^*_2SmH}$_2$]-mediated PhMCP ring-opening polymerization, while the alternative mechanism (see cycle **II** in Scheme 1) is entirely precluded, which is consistent with mechanistic data derived from experimental studies (see Introduction), and 2) not the insertion but the ring-opening step discriminates between the two conceivable mechanisms.

Among the two regioisomeric pathways for ring opening by cleavage of a proximal cyclopropyl bond, the **2a**″→**4j**′ pathway that is facilitated by a coordinating interaction of the electrophilic Sm atom with the π system of the adjacent phenyl ring is kinetically most easy ($\Delta G^{\ddagger}_{tot}=0.1$ kcal mol^{-1}), while generation of **4r**′ must overcome a barrier that is 4.6 kcal mol^{-1} higher ($\Delta\Delta G^{\ddagger}_{tot}$). The weakly Lewis basic phenyl substituent acts, by its ability to stabilize electronically the electrophilic Lewis acidic lanthanide center (which can be counterbalanced by steric factors for catalysts that are sterically congested), to control the regioselectivity of the ring-opening step, and thereby to determine the outcome of the chain-initiation process. The computed kinetic gap ($\Delta\Delta G^{\ddagger}_{tot}=4.6$ kcal mol^{-1}) argues that **4j**′ is the ring-opened regioisomer that is almost exclusively formed in the

chain-initiation process; its generation is furthermore thermodynamically favored as well. Marks et al. reported for Sm-mediated PhMCP/ethylene copolymerization a ratio of about 60:30 for entering the alternative pathways (in favor of the pathway that is related to **2a″**→**4j**) and further demonstrated that this ratio is highly sensitive to steric factors.[7b] Thus, these experimental observations in combination with the present theoretical mechanistic study strongly argue that for the [{Cp^*_2SmH}$_2$]-catalyzed PhMCP (co)polymerization, ring opening exhibits a preference for the pathway that is assisted by the phenyl substituent for both chain initiation and polymer growth. The kinetic balance between the two alternative pathways is of course also affected by steric factors. The unfavorable steric interactions of the growing polymer chain with the Cp^*_2Sm backbone, which are accounted for to only a certain extent by the employed model catalyst and, furthermore, are likely to be amplified during polymer growth, might lead to a diminished or even inverted $\Delta\Delta G^{\neq}_{tot}$ gap and thereby modulate the regioselective outcome of the polymerization process.

The β-H elimination commencing from the ring-opened products is predicted to be distinctly more expensive kinetically than the facile insertion and ring-opening processes. Formation of the two possible 1-phenyl- and 2-phenylbutadiene regioisomers is an endergonic process that exhibits very similar kinetics ($\Delta G^{\neq} = 14.3$–16.4 kcal mol^{-1}). This indicates that ring-opening isomerization is a less likely process for both kinetic and thermodynamic reasons. In agreement with this conclusion, NMR spectroscopic characterization of the PhMCP/ethylene copolymer did not reveal any indications for formation of 1,3-diene units.[7b] The higher thermodynamic population of the precursor **4j′** suggests that isomerization, if occurring at all, would give rise to 1-phenylbutadiene as the predominantly formed ring-opened PhMCP isomer.

Conclusion

Herein is presented, to the best of my knowledge, the first detailed theoretical mechanistic investigation of alternative mechanisms for chain initiation of organolanthanide-mediated ring-opening polymerization of 2-phenyl-1-methylenecyclopropane with an archetypical [Cp_2SmH] model catalyst. Several conceivable pathways for the crucial elementary processes, including ring-opening isomerization of PhMCP to phenylbutadienes, were critically scrutinized for a tentative course of the catalytic reaction (Scheme 1) by means of a gradient-corrected DFT method. The present computational study provides, for the first time, detailed insight into the intimate aspects of the process, in terms of located key structures and the free-energy profile for individual elementary steps.

The mechanism found to be operative starts with the first 1,2-insertion of the exocyclic C=C bond into the Sm−H bond and is followed by ring opening through cleavage of a proximal cyclopropyl bond (see cycle **I** in Scheme 1), while the alternative mechanism that commences with 2,1-insertion (see cycle **II** in Scheme 1) is almost entirely precluded kinetically. This is consistent with mechanistic data derived from experimental studies on the chain-growth process. Not the facile and irreversible insertion step, which does not proceed in a regioselective fashion, but the subsequent ring-opening process discriminates between the alternative mechanisms for chain initiation. Opening of the cyclopropyl ring in the 1,2-insertion product species is kinetically easy and occurs readily in an exergonic process, while a prohibitively large barrier is associated with ring opening of the 2,1-products. The ring-opened species generated along the operative mechanistic cycle can undergo further β-H elimination to afford phenylbutadienes as ring-opened isomers of PhMCP. The ring-opening isomerization, however, is predicted to be a less likely process for both kinetic and thermodynamic reasons. Among the two regioisomers, this process, if it occurs at all, would give rise to 1-phenylbutadiene.

The phenyl group was shown to discriminate between alternative pathways conceivable for each of the elementary steps. Steric factors are effective for the insertion step occurring in either 1,2- or 2,1-fashion, and thus the *anti* pathway, with the phenyl substituent in remote location, is kinetically preferred. The ring-opening process, however, is assisted by a stabilizing electronic interaction of the arene π system with the electrophilic lanthanide center. Consequently, the pathway with the phenyl group adjacent to the metal center becomes facilitated among the two regioisomeric pathways, both kinetically and thermodynamically, and hence cyclopropyl ring opening proceeds regioselectively.

The present study represents the first part of a systematic computational exploration of crucial structure–reactivity relationships in organolanthanide-assisted ROZP of methylenecycloalkanes. Overall, chain initiation of the samarocene-mediated ring-opening polymerization of PhMCP is predicted to be a smooth, kinetically facile process. On the other hand, experiments have not succeeded thus far in accomplishing PhMCP homopolymerization with this catalyst,[7b] and this suggests that the sequential insertion and ring-opening processes along the course for chain growth are energetically more expensive. The fine mechanistic details of PhMCP enchainment will be addressed in forthcoming investigations.

Acknowledgements

I wish to thank Professor Tom Ziegler (University of Calgary, Canada) for his generous support. Excellent service by the computer centers URZ Halle and URZ Magdeburg is gratefully acknowledged.

[1] a) P. Binger, H. M. Buch, *Top. Curr. Chem.* **1987**, *135*, 77; b) U. M. Dzhemilev, R. I. Khusnutdinov, G. A. Tolstikov, *J. Organomet. Chem.* **1991**, *409*, 15; c) T. Ohta, H. Takaya in *Comprehensive Organic Synthesis*, *Vol. 5*, (Ed.: B. M. Trost), Pergamon, Oxford, **1991**, p. 1185.

[2] P. von R. Schleyer, J. E. Williams, K. R. Blanchard, *J. Am. Chem. Soc.* **1970**, *92*, 2377.

[3] a) M. Lautens, W. Klute, W. Tam, *Chem. Rev.* **1996**, *96*, 49; b) I. Nakamura, Y. Yamamoto, *Adv. Synth. Catal.* **2002**, *344*, 111.
[4] a) R. Noyori, H. Takaya, *J. Chem. Soc. Chem. Commun.* **1969**, 525; b) S. Bräse, A. de Meijere, *Angew. Chem.* **1995**, *107*, 2741; *Angew. Chem. Int. Ed. Engl.* **1995**, *34*, 2545; c) M. Lautens, C. Meyer, A. Lorenz, *J. Am. Chem. Soc.* **1996**, *118*, 10676; d) N. Tsukada, A. Shibuya, I. Nakamura, Y. Yamamoto, *J. Am. Chem. Soc.* **1997**, *119*, 8123; e) D. H. Camacho, I. Nakamura, S. Saito, Y. Yamamoto, *Angew. Chem.* **1999**, *111*, 3365; *Angew. Chem. Int. Ed.* **1999**, *38*, 3365; f) M. Suginome, T. Matsuda, Y. Ito, *J. Am. Chem. Soc.* **2000**, *122*, 11015; g) M. Itazaki, Y. Nishihara, K. Osakada, *J. Org. Chem.* **2002**, *67*, 6889.
[5] For the synthesis of MCPs, see: A. Brandi, A. Goti, *Chem. Rev.* **1998**, *98*, 589.
[6] a) X. Yang, L. Jia, T. J. Marks, *J. Am. Chem. Soc.* **1993**, *115*, 3392; b) X. Yang, A. M. Seynam, P.-F. Fu, T. J. Marks, *Macromolecules* **1994**, *27*, 4625; c) L. Jia, X. Yang, S. Yang, T. J. Marks, *J. Am. Chem. Soc.* **1996**, *118*, 1547; d) L. Jia, X. Yang, A. M. Seyam, I. D. L. Albert, P.-F. Fu, S. Yang, T.-J. Marks, *J. Am. Chem. Soc.* **1996**, *118*, 7900.
[7] a) T. R. Jensen, T. J. Marks, *Macromolecules* **2003**, *36*, 1775; b) T. R. Jensen, J. J. O'Donnell, III, T. J. Marks, *Organometallics* **2004**, *23*, 740; c) typical reaction conditions for organolanthanide-catalyzed ring-opening polymerization of methylenecycloalkanes are 25 °C in noncoordinating solvents (benzene, toluene, and pentane).
[8] a) D. Takeuchi, S. Kim, K. Osakada, *Angew. Chem.* **2001**, *113*, 2757; *Angew. Chem. Int. Ed.* **2001**, *40*, 2685; b) S. Kim, D. Takeuchi, K. Osakada, *J. Am. Chem. Soc.* **2002**, *124*, 762; c) S. Kim, D. Takeuchi, K. Osakada, *Macromol. Chem. Phys.* **2003**, *204*, 666; d) D. Takeuchi, K. Anada, K. Osakada, *Angew. Chem.* **2004**, *116*, 1253; *Angew. Chem. Int. Ed.* **2004**, *43*, 1233.
[9] a) P. L. Watson, G. W. Parshall, *Acc. Chem. Res.* **1985**, *18*, 51; b) E. Bunel, B. J. Burger, J. E. Bercaw, *J. Am. Chem. Soc.* **1988**, *110*, 976; c) J. W. Eshuis, Y. Y. Tan, J. H. Teuben, *J. Mol. Catal.* **1990**, *62*, 277; d) L. Resconi, F. Piemontesi, G. Franciscono, L. Abis, T. Fiorani, *J. Am. Chem. Soc.* **1992**, *114*, 1025; e) X. Yang, C. Stern, T. J. Marks, *J. Am. Chem. Soc.* **1994**, *116*, 10015.
[10] For examples of (η^3-allyl)Cp^*_2Ln complexes, see: a) S. P. Nolan, C. Stern, T. J. Marks, *J. Am. Chem. Soc.* **1989**, *111*, 7844; b) A. Scholz, A. Smola, J. Scholz, J. Löbel, H. Schimann, K.-H. Thiele, *Angew. Chem.* **1991**, *103*, 444; *Angew. Chem. Int. Ed. Engl.* **1991**, *30*, 435; c) W. J. Evans, R. A. Keyer, G. W. Rabe, D. K. Drummond, J. W. Ziller, *Organometallics* **1993**, *12*, 4664; d) W. J. Evans, S. L. Gonzales, J. W. Ziller, *J. Am. Chem. Soc.* **1994**, *116*, 2600; e) F. T. Edelmann, *Top. Curr. Chem.* **1996**, *179*, 247; f) *Topics in Organometallic Chemistry*, *Vol. 2*, (Ed.: S. Kobayashi), Springer, Berlin, **1999**.
[11] a) Y. Luo, P. Selvam, Y. Ito, S. Takami, M. Kubo, A. Imamura, A. Miyamoto, *Organometallics* **2003**, *22*, 2181; b) Y. Luo, P. Selvam, A. Endou, M. Kubo, A. Miyamoto, *J. Am. Chem. Soc.* **2003**, *125*, 16210; c) As the specific details of the employed computational approach were not completely reported by these authors, we are not in the position to provide any explanation of the origin of the striking difference in the predicted energy profiles for the insertion and ring-opening steps between the present and past investigations. The BP86/SDD-TZVP energetics reported in the present study, however, were confirmed for each of the individual elementary processes at the B3LYP/SDD-TZVP level (see Supporting Information), so there is confidence that the energetic aspects herein are described adequately.
[12] a) R. Ahlrichs, R. , M. Bär, M. Häser, H. Horn, C. Kölmel, *Chem. Phys. Lett.* **1989**, *162*, 165; b) O. Treutler, R. Ahlrichs, *J. Chem. Phys.* **1995**, *102*, 346; c) K. Eichkorn, O. Treutler, H. Öhm, M. Häser, R. Ahlrichs, *Chem. Phys. Lett.* **1995**, *242*, 652.
[13] a) P. A. M. Dirac, *Proc. Cambridge Philos. Soc.* **1930**, *26*, 376; b) J. C. Slater, *Phys. Rev.* **1951**, *81*, 385; c) S. H. Vosko, L. Wilk, M. Nussiar, *Can. J. Phys.* **1980**, *58*, 1200; d) A. D. Becke, *Phys. Rev. A* **1988**, *38*, 3098; e) J. P. Perdew, *Phys. Rev. B* **1986**, *33*, 8822; J. P. Perdew, *Phys. Rev. B* **1986**, *34*, 7406.
[14] see, for instance: a) H. Heiber, O. Gropen, J. K. Laerdahl, O. Swang, U. Wahlgren, *Theor. Chim. Acta* **2003**, *110*, 118; b) S. Tobisch, Th. Nowak, H. Boegel, *J. Organomet. Chem.* **2001**, *619*, 24.
[15] M. Dolg, H. Stoll, A. Savin, H. Preuß, *Theor. Chim. Acta* **1989**, *75*, 173.
[16] a) A. Schäfer, C. Huber, R. Ahlrichs, *J. Chem. Phys.* **1992**, *97*, 2571; b) A. Schäfer, C. Huber, R. Ahlrichs, *J. Chem. Phys.* **1994**, *100*, 5829.
[17] W. Koch, M. C. Holthausen, *A Chemist's Guide to Density Functional Theory*, 2nd ed., Wiley-VCH, Weinheim, **2001**.
[18] D. A. McQuarrie, *Statistical Thermodynamics*, Harper & Row, New York, **1973**.
[19] a) C. J. Cramer, D. G. Truhlar, *Chem. Rev.* **1999**, *99*, 2161; b) C. J. Cramer, E *ssentials of Computational Chemistry: Theories and Models*, Wiley, Chichester, **2002**, pp. 347–383.
[20] a) A. Klamt, G. Schüürmann, *J. Chem. Soc. Perkin Trans. 2* **1993**, 799; b) A. Klamt, In *Encyclopedia of Computational Chemistry*, *Vol. 1*, (Ed.: P von R. Schleyer), Wiley, Chichester, **1998**, pp. 604–615.
[21] A. Schäfer, A. Klamt, D. Sattel, J. C. W. Lohrenz, F. Eckert, *Phys. Chem. Chem. Phys.* **2000**, *2*, 2187.
[22] *CRC Handbook of Chemistry and Physics*, 3rd electronic ed. (Ed.: D. R. Lide), **2000**; http://www.knovel.com/.
[23] A. Klamt, V. Jonas, Th. Bürger, J. C. W. Lohrenz, *J. Phys. Chem. A* **1998**, *102*, 5074.
[24] E. Wilhelm, R. Battino, *Chem. Rev.* **1973**, *73*, 1.
[25] J. Cooper, T. Ziegler, *Inorg. Chem.* **2002**, *41*, 6614.
[26] For further details, see www.struked.de.
[27] For examples of lanthanide arene complexes, see: a) H. Schuman, J. A. Meese-Marktscheffel, L. Esser, *Chem. Rev.* **1995**, *95*, 865; b) M. N. Bochkarev, *Chem. Rev.* **2002**, *102*, 2089.
[28] See for instance: P. Margl, L. Deng, T. Ziegler, *J. Am. Chem. Soc.* **1998**, *120*, 5517.
[29] There is substantial precedent for η^n-benzylic structures in organo f element chemistry. See for instance: a) W. J. Evans, T. A. Ulibarri, J. W. Ziller, *J. Am. Chem. Soc.* **1990**, *112*, 219; b) E. A. Minitz, K. G. Moley, T. J. Marks, V. W. Day, *J. Am. Chem. Soc.* **1982**, *104*, 4692; c) M. A. Giardello, V. P. Conticello, L. Brard, M. R. Gagne, T. J. Marks, *J. Am. Chem. Soc.* **1994**, *116*, 10241; d) P.-F. Fu, L. Brard, Y. Li, T. J. Marks, *J. Am. Chem. Soc.* **1995**, *117*, 7157; e) G. A. Molander, J. A. C. Romero, C. P. Corrette, *J. Organomet. Chem.* **2002**, *647*, 225.
[30] This is indicated by examining the process in a linear transit approach, although we were not able to locate the corresponding transition state.
[31] The bimolecular insertion is the only step in the investigated sequence of processes for which free energies depend on the applied scaling factor (two-thirds) of the computed gas-phase entropies. A smaller factor (for instance, one-half) reduces the free-energy barrier to 4.0 and 5.0 kcal mol^{-1} for the feasible *anti* pathway for 1,2- and 2,1-insertion, respectively. The energetic gap between the regioisomeric insertion events ($\Delta\Delta G^{\ddagger} = 1.0$ kcal mol^{-1}) and mechanistic conclusions are not at all affected by the scaling factor.

Received: November 1, 2004
Published online: March 15, 2005